DOI: 10.61782/fa.2025.0680

FORUM ACUSTICUM
EURONOISE 2025

PERIODIC BOUNDARY CONDITIONS IN FINITE DIFFERENCE TIME DOMAIN

Jaime Galiana-Nieves[1*] **Rubén Picó**[1,2]
David Ramírez-Solana[2,3] **Javier Redondo**[1,2]
[1] Universitat Politècnica de València, Valencia, Spain
[2] Instituto de Investigación para la Gestión Integrada de zonas Costeras, Gandía, Spain
[3] Structured Materials and Dynamics Lab, School of Civil Engineering, University College Dublin, Ireland

ABSTRACT

Finite difference time domain (FDTD) is a numerical technique that has been well-established for cases where the time signature of an acoustic system is required. As with other volumetric methods, it involves discretely meshing the full spatial domain under study. In the case of periodic structures, such as sonic crystals, periodic boundary conditions can be used to minimise the computational cost of the simulation, since they allow for the consideration of an infinite number of periodic elements. The normal incidence case is straightforward; however, a number of incidence angles are required for the proper characterisation of a periodic material. There are several methods for implementing periodic boundary conditions with varying incident angles, each with its advantages and disadvantages. In this work, we present a review of the aforementioned techniques and compare their performance in a particular case.

Keywords: *FDTD, Periodic Boundary Conditions, Sonic Crystals, Sound Reduction*

1. INTRODUCTION

Noise, defined as unwanted sound from human activities, negatively impacts health and quality of life [1]. When source mitigation is unfeasible, noise barriers (NBs) are commonly used during the transmission phase [2]. To plan solutions with NBs, it is essential to understand their acoustic properties, especially their insulation. There are two standards for measuring insulation: EN 1793-2:2019 [3] (referred to as diffuse incidence), which is conducted in a laboratory with a diffuse sound field, and EN 1793-6:2019+A1:2022 [4] (or in situ method), which is applied directly at the installation site with normal incidence. Although the in situ method has gained popularity due to its direct applicability, the laboratory method is still used in countries like Spain and Portugal because of the accumulated experience and the complexity of the post-processing required by the second method.

Both methods assume very different incidence conditions: diffuse in the first, normal in the second. However, in real-life situations—such as roads or railway tracks—the sound strikes the barrier in a plane. Therefore, a third method, called Flat Average, is proposed to reflect this realistic incidence.

Traditional NBs, made of dense, rigid materials, reflect, diffract, or absorb sound energy [5], but they lack permeability, aesthetic appeal, and frequency selectivity [6]. To overcome these limitations, Sonic Crystal Noise Barriers (SCNBs) have been proposed. These structures rely on Bragg interference from multiple scattering (MS), which generates frequency-dependent attenuation bands called Bragg band gaps (Bragg-BGs), determined by the lattice constant [7]. The concept was introduced theoretically by Kushwaha in 1997 [8] and experimentally validated by Sánchez-Pérez in 2002 using arrays of rigid

*__Corresponding author__: jaiganie@doctor.upv.es.

cylinders [9].

As will be shown later, the differences between previously methods are small when the insulation varies little with the angle, like the case of traditional NBs. However, in devices with strong angular dependence—such as SCNB—the discrepancies between methods can be significant.

In the present work, the results of the three insulation measurement techniques previously mentioned are compared through numerical simulation, both for homogeneous screens and SCNB. The following section will present the numerical technique used, section 3 will cover the calculations of the insulation for each of the three methods, and section 4 will describe the simulation models. Section 5 will show the results, and finally, section 6 will present the conclusions drawn.

2. OBLIQUE INCIDENCE IN FDTD

The finite differences time domain method (FDTD) was first introduced in electromagnetics [10] to study wave propagation and was later adapted to acoustic wave evaluation [11]. It comes from the discretizations of the mass and momentum equations, discretized in time and space and staggering the grids of acoustic pressure and particle velocity. For the acoustic pressure p, we define a set of two different components p_x and p_y. This separation serves the purpose of implementing Perfectly Matched Layers (PMLs) that reduce the unwanted reflections on the boundaries of the system.

$$p_{x}{}^{n}_{(i,j)} = p_{x}{}^{n-1}_{(i,j)} - \frac{\rho_0 c_0^2 \Delta t}{\Delta x}\left(u_{x}{}^{n-1/2}_{(i+1/2,j)} - u_{x}{}^{n-1/2}_{(i-1/2,j)}\right) \quad (1)$$

$$p_{y}{}^{n}_{(i,j)} = p_{y}{}^{n-1}_{(i,j)} - \frac{\rho_0 c_0^2 \Delta t}{\Delta y}\left(u_{y}{}^{n-1/2}_{(i,j+1/2)} - u_{y}{}^{n-1/2}_{(i,j-1/2)}\right) \quad (2)$$

$$p^n = p_x^n + p_y^n. \quad (3)$$

Here, n is the time step in which the simulation is updated. Each time step represents an advance of Δt seconds in time. The mesh precision comes defined by the distance between grid points in each direction, Δx and Δy. Each pressure or velocity point is in a position defined by $i\Delta x$ and $j\Delta y$. The sound particle velocity is then updated in a similar manner:

$$u_{x}{}^{n+1/2}_{(i+1/2,j)} = u_{x}{}^{n-1/2}_{(i+1/2,j)} - \frac{\Delta t}{\rho_0 \Delta x}\left(p^n_{(i+1,j)} - p^n_{(i,j)}\right) \quad (4)$$

$$u_{y}{}^{n+1/2}_{(i,j+1/2)} = u_{y}{}^{n-1/2}_{(i,j+1/2)} - \frac{\Delta t}{\rho_0 \Delta y}\left(p^n_{(i,j+1)} - p^n_{(i,j)}\right). \quad (5)$$

It can be observed that the velocity points u_x and u_y are both staggered in time and space by a factor of $1/2$. Particle velocity in each direction. After iteratively updating the pressure and velocity fields using Eqs. (1) to (5), the propagation of sound waves in the medium can be obtained. The values of the medium density ρ and propagation speed c can be a function of the position within the model. Altogether with the boundary conditions designed for these models, it can perform accurate simulations of wave propagation through complex models.

To study the propagation of sound through infinite periodic or semi-infinite structures its necessary to implement periodic boundary conditions on the limits of the model to emulate an infinite structure. This can be easily done for normal incidence by just substituting the edge values on the periodic direction with those from the opposite side. The problem arises when the wave impinges the structure presents a non-normal incidence. There are some methods that can be used to study those cases. In this work we are going to focus on three different methods for the implementation of FDTD simulations with periodic boundary conditions for the study of periodic structures with different angles of incidence. The main issue with the implementation of periodic boundary conditions with non-normal angles of incidence resides in the need of *future* instants of the wave propagating through the model to achieve the periodicity. Since it is not possible to predict the future characteristics of a wave propagating through complex media, some methods have been developed to avoid this problem [12].

2.1 Multiple Unit Cells

One of the methods widely used for the study of periodic structures with different angles of incidence is the Multiple Unit Cells method. Given a periodic structure, a model made of a series of rows of this structure is implemented. The amount of rows has to be enough for the

periodicity effects to be observed. The boundaries of the model, except the one at the top, are designed with absorbing boundary conditions. In this case, the boundary at the top is where the process to obtain the periodicity of the model is applied.

If we have an incident wave with an angle of incidence of θ, the time delay between the particle velocity at the top boundary and the y position at the beginning of the last row of the periodic structure is

$$t_d = y_c \sin\theta / c_0, \tag{6}$$

where y_c is the thickness of the individual periodic row and c_0 is the propagation speed in the medium.

To implement the periodicity using this method, we inject in the top row of particle velocities in the y direction the particle velocity in the first row of the final periodic subdivision and apply the time delay defined. This can be expressed as

$$u_y(x, y_{top}, t) = u_y(x, y_{top} - y_p, t - t_d), \tag{7}$$

where u_y is the particle velocity in the y direction, y_{top} is the y position of the last row of the system and t is the instant of the model update. The excitation chosen for this method is a wide band Ricker wavelet with a time delay applied for every position in the y direction that allows the wave to propagate with the desired angle of incident. This also means that this model is capable of evaluate a great number of frequencies for each angle of incidence. For the evaluation of the model, only the results at the upper set of scatterers is taken into account.

2.2 Sine-Cosine Method

The Sine-Cosine method is a single frequency approach to the periodic problem. Similar to the Multiple Unit Cells method, it relies on a delay applied to the periodic boundaries of the model. However, since the model evaluated is conformed by a single row of scatterers, the implementation needs to be carefully adjusted.

To properly implement periodic boundary conditions, it has to affect both the top and bottom limits of the model. Given an angle of incidence θ, the wave propagating at the top line of the model is delayed by a time t_d as defined in Equation 6. The issue appears in the implementation of the periodicity for the bottom row, which has to be a future value of the sound velocity in the top row. Since we can not predict future values of the sound velocity in these cases, a phase shift is applied to create these conditions. This can be made if the excitation is defined by a single frequency. This phase shift is defined as

$$\hat{\omega} = e^{i\frac{2\pi f}{c_0} y_c \sin\theta}, \tag{8}$$

where y_c is the length of the model in the y direction and f is the excitation frequency.

When updating the model, the velocity points on the edges of the system need to be evaluated by applying the defined phase shift. For the lower row of particle velocity in y the update equation is defined as follows

$$u_y^{n+1/2}(i, -1/2) = u_y^{n-1/2}(i, -1/2) - \frac{\Delta t}{\rho_0 \Delta y}\left(p(i,0)^n - p(i, y_c)\hat{\omega}\right). \tag{9}$$

It can be observed that the phase shift $\hat{\omega}$ is applied to the upper row of sound pressure values to add them below the lower velocity points in the y direction to implement a boundary condition which causes a continuum in the model that depends on the frequency and the angle of the incident wave. As for the update equations of the upper velocity row, it is important to conjugate the phase shift, so for this case the wave needs to be "delayed" in order to fulfill the periodicity condition:

$$u_y^{n+1/2}(i, y_c + \Delta y/2) = u_y^{n-1/2}(i, y_c + \Delta y/2) - \frac{\Delta t}{\rho_0 \Delta y}\left(p(i,0)^n \hat{\omega}^* - p(i, y_c)\right) \tag{10}$$

This method allows the evaluation of periodic structures with different angles of incidence utilizing way smaller grids than the Multiple Cell method. However, since it only allows to study one frequency at a time it is needed to run a number of simulations in order to obtain a precise response of the structure under study.

2.3 Mapped Field Method

The last method studied in this work is the Mapped Field Method. This method comes from the Field Transformation Techniques proposed in electromagnetism to study wave propagation through periodic structures with broadband results for each angle of incidence. For that purpose, it is needed to modify the update equations of the classical FDTD method [13].

First of all, a series of auxiliary variables are defined to eliminate the phase shift caused by the angle of incidence. This phase shift comes from the fact that the wave vector in the x and y directions depend on said angle of

incidence. For that purpose, that phase shift is added to the initial values of pressure and particle velocity. Assuming we have a periodicity set in the y direction, the new pressure and velocity expressions result in

$$P = pe^{-ik\sin\theta y}, \tag{11}$$

$$V = ue^{-ik\sin\theta y}. \tag{12}$$

where k is the wavenumber defined as $k = \omega/c_0$ and y is the position in the vertical direction. Substituting these new values in the original wave equations and properly discretizing we obtain a new set of update equations.

$$\hat{V}_{y(i,j+1/2)}^{\,n+1} = \hat{V}_{y(i,j+1/2)}^{\,n-1} - \frac{2\Delta t}{\rho_0 \Delta y}\left(P_{i,j+1}^{n} - P_{i,j}^{n}\right) \tag{13}$$

$$V_{x(i+1/2,j)}^{\,n+1} = V_{x(i+1/2,j)}^{\,n-1} - \frac{2\Delta t}{\rho_0 \Delta y}\left(P_{(i+1,j)}^{n} - P_{(i,j)}^{n}\right) \tag{14}$$

$$\hat{P}_{y(i,j)}^{\,n+1} = \hat{P}_{y(i,j)}^{\,n-1} - \frac{2\Delta t c_0^2 \rho_0}{\Delta y}\left(V_{y(i,j+1/2)}^{\,n} - V_{y(i,j-1/2)}^{\,n}\right) \tag{15}$$

$$P_{x(i,j)}^{\,n+1} = P_{x(i,j)}^{\,n-1} - \frac{2\Delta t c_0^2 \rho_0}{\Delta y}\left(V_{x(i+1/2,j)}^{\,n} - V_{x(i-1/2,j)}^{\,n}\right) \tag{16}$$

$$P_{y(i,j)}^{\,n+1} = (\hat{P}_{y(i,j)}^{\,n+1} + c_0\rho_0\left(\frac{\hat{V}_{y(i,j+1/2)}^{\,n+1} + \hat{V}_{y(i,j-1/2)}^{\,n+1}}{2}\right) + P_{x(i,j)}^{\,n+1}\sin^2\theta)/\left(1-\sin^2\theta\right) \tag{17}$$

$$P_{(i,j)}^{n+1} = P_{x(i,j)}^{\,n+1} + P_{y(i,j)}^{\,n+1} \tag{18}$$

$$V_{y(i,j+1/2)}^{\,n+1} = \hat{V}_{y(i,j+1/2)}^{\,n+1} + \frac{1}{c_0\rho_0}\frac{P_{(i,j+1)}^{n+1} + P_{(i,j)}^{n+1}}{2}\sin\theta \tag{19}$$

This new set of variables are divided in two main groups. The first one are the pressure variables, composed by the global acoustic pressure P, the acoustic pressure in the x direction P_x, the acoustic pressure in the y direction P_y and the auxiliary pressure needed to implement the method without taking into account the frequency dependence of the equations $\hat{P}_y$. The second group of velocity values follow the same notation.

It can be observed that all the equations are updated in the same instant $n+1$. This simultaneous updating cannot be achieved with classic leapfrog FDTD scheme. That is the reason why the variation of FDTD Centered in Time (CIT-FDTD) has been utilized for the implementation of this method. That variation synchronizes the update of all the variables with the cost of having to save an additional time step to perform the discrete derivative through two iterations. This method allows us to obtain a broadband response of a periodic structure for each angle of incidence using a single row of scatterers with a simple periodicity set on its boundaries.

3. EVALUATION OF THE SOUND INSULATION

In real studies, mainly two measuring techniques are used to assess the isolation provided by any type of barrier. The normal incidence measurement, also known as *in situ* measurements, and the diffuse field method, performed in transmission chambers under laboratory conditions. Another way of measuring the real transmission of a barrier would be to average the transmission for each angle of incidence equally, since in real conditions the sound incident to the barrier will have the same importance regardless of the angle of incidence [3, 4, 14].

3.1 Diffuse field

Under laboratory conditions, the isolation provided by a barrier is assessed by applying a diffuse field onto the surface of the barrier. The statistical model that defines the relevance of each angle of incidence under diffuse field conditions can be described using the Paris formula [15], resulting in a global transmission coefficient of

$$\tau(f) = \frac{1}{\varphi_{max}} \frac{\int_0^{\theta_{max}}\int_0^{\varphi_{max}} \tau(\theta,\varphi,f)\sin\theta\cos\theta d\phi d\theta}{\int_0^{\theta_{max}}\int_0^{\varphi_{max}} \sin\theta\cos\theta d\phi d\theta} \tag{20}$$

where a global transmission coefficient $\tau(f)$ is obtained from averaging the angle dependent transmission coefficient $\tau(\theta,\varphi,f)$ through with all possible angles of incidence.

3.2 *In situ* measurements

One of the most widely used methods of characterization of acoustic barriers is the *in situ* method. This procedure only takes into account the normal incidence when it comes to assessing the insulating characteristics of a barrier. Thus, this method does not take into account the range of angles of incidence that can act on the barrier in a real situation.

3.3 Simple average

Under real conditions, barriers are not usually surrounded by diffuse field conditions. However, the barrier prevents the sound to reach the receiving point regardless of the incidence angle. This is the case for linear sound sources such as roads or train tracks. If each sound source if assumed to be incoherent with the others, it is possible to calculate the overall intensity that reaches the receiver as the sum of each differential element of the linear source. Without taking into account the sound attenuation caused by the propagation through air, each differential element will provide a sound intensity defined as dI which will be proportional to the inverted distance from that element to the receiver

$$dI = \frac{I_0}{r} dy = \frac{I_0}{x^2 + y^2} dy \tag{21}$$

where I_0 is proportional to the sound power per length of the sound source. The total intensity at the receiver can be calculated as

$$I = \int \frac{I_0}{x^2 + y^2} dy. \tag{22}$$

To solve this, a variable switch can be made in a way that

$$y = x \tan\theta \tag{23}$$

$$\sqrt{x^2 + y^2} = \frac{x}{\cos\theta} \tag{24}$$

finally obtaining that

$$I = \int \frac{I_0}{x} d\theta. \tag{25}$$

Both I_0 and x are constant values. The integration limits for the angle of incidence apply to every possible angle and so it is defined as $[-\pi/2, \pi/2]$. We finally obtain that the overall intensity is proportional to the inversion of the distance to the nearest point of the lineal source. So this translates to the conclusion that every angle is equally relevant when assessing the transmission coefficients of a barrier placed next to a linear source.

4. SIMULATED MODELS

For the purpose of validating the simulation methods and obtaining the sound insulation provided by barriers made by periodic structures, two sets of simulations were implemented. All simulations are 2-dimensional.

4.1 Thin layers

The transmission coefficient of an homogeneous layer with a density different of airs but the same propagation speed is known theoretically [16] and can be obtained by the following formula:

$$\tau = \frac{1}{1 + \frac{1}{4}\left(Z_2/Z_1 - Z_1/Z_2\right)^2 \sin^2(kL\cos\theta)} \tag{26}$$

where Z_1 and Z_2 are the acoustic impedance of the medium surrounding the layer and the impedance of the layer respectively. The wavenumber inside the medium k gets modified by the angle of the incident wave θ. Finally, the thickness L of the barrier allows us to obtain the behavior of the system.

For each simulation technique described, we have obtained the results for an homogeneous layer with a thickness $L = 0.2m$ and a density $\rho = 10\rho_0$, being ρ_0 the density of air.

The matching of the results from the simulations and the theoretical results can help us validate the simulation models to obtain the sound transmission coefficient of more complicated systems.

4.2 Sonic crystals

Our main objective of this work is to properly assess the sound insulation provided by sonic crystals and so, a set of numerical simulations has been performed to study the results from the aforementioned evaluation procedures. The periodic structures simulated are identical for each simulation method previously described: a sonic crystal formed by three cylindrical scatterers periodically repeated. The distance between the center of each scatterer, also known as the lattice constant is defined as $l_c = 0.17m$ and each scatterers have a diameter of $d = 0.75l_c$.

5. RESULTS

In this section we present the results obtained with the 3 methods under analysis.

5.1 Homogeneous layer

First we observe the results for an homogeneous layer of thickness $L = 0.2m$ and a density $\rho = 10\rho_0$ with $\rho_0 = 1.21kg/m^3$. In Figure 1 it shows the sound reduction index provided by such a barrier at normal incidence with each simulation method and compared with the theoretical result provided by Eq (26). It shows a

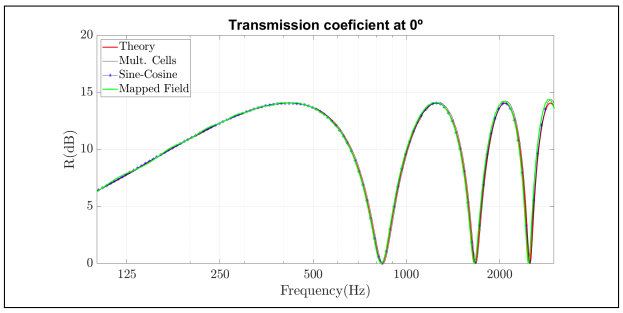

Figure 1. Sound reduction index provided by a layer of dense material with a density 10 times that of airs and a thickness of 0.2m at normal incidence. The theoretical result (red) is compared with those from the simulations: Multiple Unit Cells (black), Sine-Cosine Method (blue), Mapped Field Method (green).

proper matching between the three simulation techniques and the theoretical results. However, if we increase the angle of incidence as shown in Figure 2 to 30º we start to observe a subtle mismatch between the Multiple Unit Cells Method and the rest of results. This is more noticeable the bigger the angle. As in Figure 3, with an angle of incidence of 75º, the Multiple Unit Cells method suffers a severe frequency shift as well as an important ammount of numerical noise. The sine-cosine method also deviates from the theoretical solution, but not in a unassimilable way. It has been observed that the Multiple Unit Cells

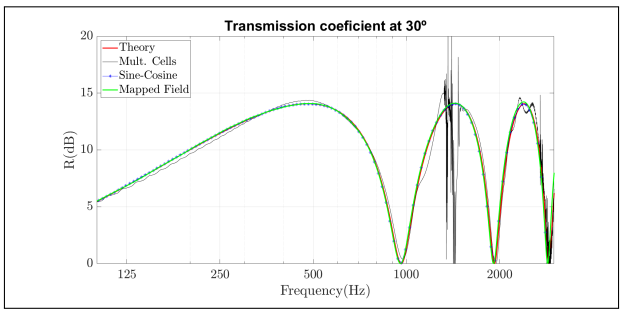

Figure 2. Sound reduction index provided by a layer of dense material with a density 10 times that of airs and a thickness of 0.2m with an angle of incidence of 30º.

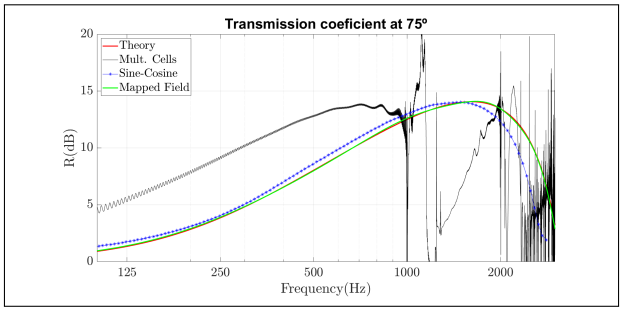

Figure 3. Sound reduction index provided by a layer of dense material with a density 10 times that of airs and a thickness of 0.2m with an angle of incidence of 75º.

method falls apart at great angles of incidence. For that reason, only the Sine-Cosine and Mapped Field methods are taken into account to obtain the different transmission coefficients by means of the procedures described in section 3. In Fig.4 we can observe the different assessment results for the theoretical solution, the sine-cosine method and the mapped field method, showing a good agreement in every case.

5.2 Sonic crystal

After validating the simulation techniques by comparing the results with the theoretical values of a thin homogeneous layer, simulation of sonic crystals have been performed. The sound reduction index obtained by each technique is shown in Figure 5. It can be observed a good agreement between the three methods, mostly at small angles of incidence. However, the mapped field method starts to differ from the others after around a 30º incidence angle. Then, observing just the sine-cosine method and the mapped field method, we apply the aforementioned assessment aproaches to try to obtain the *real* reduction index provided by a barrier made of rigid periodic scatterers. In Figure 6 are shown the results for each assessment procedure applied to the results of both simulation techniques. We observe that the Mapped Field method provides higher values of sound reduction at high frequen-

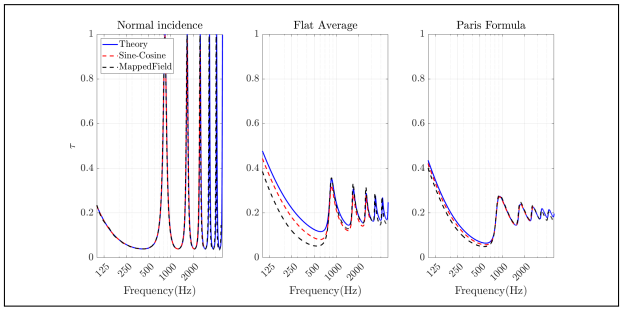

Figure 4. Comparison between different ways of assessment of the sound transmission provided by a barrier. On the left, the transmission coefficient at normal incidence. Then, the flat average as described in 3.3. Finally, on the left, the Paris formula average from 3.1. The results for the theoretical formula (red) are compared with those from the sine cosine method (dashed red) and the Mapped Field method (dashed black).

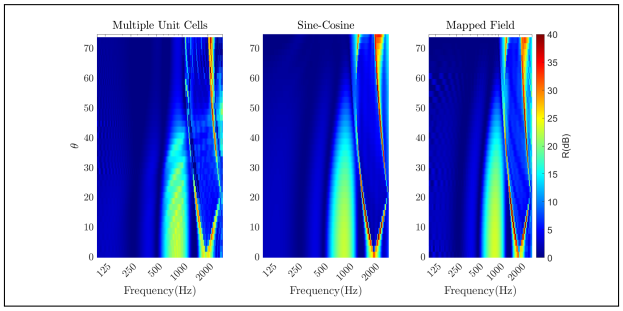

Figure 5. Color map of the sound reduction index, R, in decibels, for each of the simulation methods studied in this work for a sonic crystal made of three columns of scatterers with a lattice constant of 0.17m and a diameter of a 75% of the lattice constant. The x axis sets the frequency and the y axis is the angle of incidence θ.

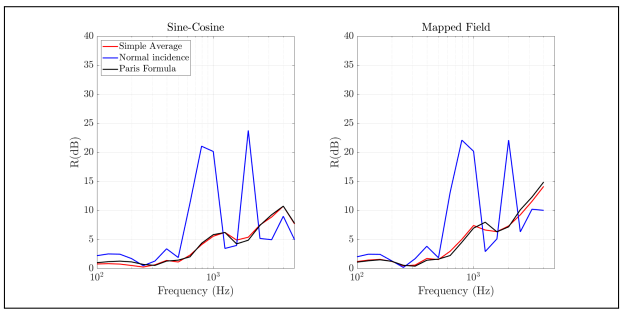

Figure 6. Comparison of the results for the sound reduction assessment of a sonic crystal by using the Sine Cosine (left) and Mapped Field methods (right). The blue line represent the results at normal incidence. The flat average is shown in red and the Paris formula averaging is shown in black,

cies. And with both techniques, the results for the flat average and the Paris formula average appear to be quite similar, showing a great difference with isolation provided at normal incidence.

6. CONCLUSIONS

In this work, we have compared three simulation techniques for obtaining sound transmission through semi-infinite periodic structures with different angles of incidence.

From the three different methods implemented, the Multiple Unit Cells method shows poor accuracy when the angle of incidence approaches large values. However, this method allows to simulate a wide band of frequencies at a time. The sine-cosine method solves the problem of the low accuracy at large angles of incidence but only one frequency can be simulated at a time, so multiple simulations need to be run for every angle of incidence.

Finally, the Mapped Field method solves both issues, allowing to analyze all the frequency range defined for each angle of incidence simulated. It only requires the definition of some auxiliary variables that increase the memory usage of the system, but it still is a fraction of that used by bigger models such as the ones used for the Multiple Unit Cells method.

Once the results for each angle of incidence were obtained, we have assessed the sound transmission with different measurement procedures. It is observed that the normal incidence measurements differ greatly from the results obtained by the two averaged methods proposed. In real life conditions, it is improbable that normal sound incidence nor diffuse field conditions are present upon a sound barrier.

From here it would be interesting to perform laboratory studies comparing each different measurement method and analyze how it compares with real life measurements. Also, the implementation of more complex simulation

models for periodic structures and other kinds of acoustic materials with periodic boundary conditions is a field that needs to be further studied.

7. ACKNOWLEDGMENTS

This work has been funded by the project PID2022-138321NB-C22 of the Spain's Ministry of Science and Innovation.

8. REFERENCES

[1] *Implementation of the Environmental Noise Directive in accordance with Article 11 of Directive 2002/49/EC*. European Comission, 2023.

[2] C. Harris, *Handbook of Acoustical Measurements and Noise Control*. McGraw-Hill,1991, 1991.

[3] *EN 1793-2: Road traffic noise reducing devices-Test methid fir determining the acoustic performance- Part 2: Intrinsic characteristics of airborne sound insulation under diffuse sound field conditions.* European Comitee for Standarisation, 2019.

[4] *EN 1793-6:Road traffic noise reducing devices-Test method for determining the acoustic performance. Part 6: In situ values of airborne sound insulation under direct sound field conditions. 2023*. European Comitee for Standarisation, 2023.

[5] *Federal Highway Administration*. United States Department of Transportation Annual Modal Research Plans Fiscal Year 2019, 2018.

[6] L.Fredianelli, L. Pizzo, and G.Licitra, "Sonic crystals as barriers for road traffic noise mitigation," *Enviroments*, vol. 6, p. 14, 2019.

[7] C. Kittel, *Introduction to Solid State Physics*. John Wiley Sons, Inc, 2005.

[8] M. Kushwaha, "Stop-bands for periodic metallic rods: Sculptures that can filter the noise," *Applied Physics*, vol. 70, pp. 3218–3220, 1997.

[9] J. Sánchez-Perez, C.Rubio, R.Martínez-Sala, R.Sánchez-Grandia, and V.Gómez, "Acoustic barriers based on periodic arrays of scatterers," *Applied Physics Letters*, vol. 81, pp. 5240–5242, 2002.

[10] K.Yee, "Numerical solution of initial boundary value problems involving maxwell's equations in isotropic media," *IEEE Transactions on Antennas and Propagation*, vol. 14, pp. 302–307, 1966.

[11] J. Redondo, R. Picó, B. Roig, and M. Avis, "Time domain simulation of sound diffusers using finite-difference schemes," *Acta Acustica united with Acustica*, vol. 93, 07 2007.

[12] A.Taflove, S. Hagness, and M.Piket-May, *Electromagnetics: The Finite-Difference Time-Domain Method, in The Electrical Engineering Handbook*. Elsevier, 2005.

[13] M. Takemura and M. Toyoda, "Analysis of the oblique incidence of periodic structures in a sound field by the finite-difference time-domain method," vol. 167, p. 107357.

[14] J. Redondo, J. Galiana-Nieves, D. Ramírez-Solana, and R. Picó, "Estándares de medida de aislamiento de pantallas acústicas: "el bueno, el feo y el malo"," in *XIII Congreso Ibérico de Acústica. 55º Congreso Español de Acústica, Tecniacústica 2024.*, 2024.

[15] E.T.Paris, "on the coefficient of sound-absorption measured by the reverberation method," *The London, Edinbrugh, and Dublin Philophical Magazine and Journal of Science*, no. 5:29, pp. 489–497, 1928.

[16] L. E.Kinsler, A. R.Frey, A. B.Coppens, and J. V.Sanders, *Fundamentals of Acoustics*. New York: John Wiley Sons, Inc, 2000.